

## Analyzing your complexes: structure of the quinol-fumarate reductase respiratory complex

Tina M Iverson\*, César Luna-Chavez†, Imke Schröder‡, Gary Cecchini† and Douglas C Rees§

The integral membrane protein complex quinol-fumarate reductase catalyzes the terminal step of a major anaerobic respiratory pathway. The homologous enzyme succinate-quinone oxidoreductase participates in aerobic respiration both as complex II and as a member of the Krebs cycle. Last year, two structures of quinol-fumarate reductases were reported. These structures revealed the cofactor organization linking the fumarate and quinol sites, and showed a cofactor arrangement across the membrane that is suggestive of a possible energy coupling function.

### Addresses

\*Graduate Option in Biochemistry, 147-75 CH, California Institute of Technology, Pasadena, CA 91125, USA

†Molecular Biology Division, Department of Veterans Affairs Medical Center, San Francisco, CA 91421 and Department of Biochemistry and Biophysics, University of California, San Francisco, CA 94143, USA

‡Department of Microbiology and Molecular Genetics, University of California, Los Angeles, CA 90095, USA

§Howard Hughes Medical Institute, Division of Chemistry and Chemical Engineering, 147-75 CH, California Institute of Technology, Pasadena, CA 91125, USA; e-mail: dcrees@caltech.edu.

Current Opinion in Structural Biology 2000, 10:448–455

0959-440X/00/\$ – see front matter

© 2000 Elsevier Science Ltd. All rights reserved.

### Abbreviations

<b>FAD</b>	flavin adenine dinucleotide
<b>PDB</b>	Protein Data Bank
<b>QFR</b>	quinol-fumarate reductase
<b>rmsd</b>	root mean square deviation
<b>SQR</b>	succinate-quinone oxidoreductase

### Introduction

Bacteria such as *Escherichia coli* can utilize multiple respiratory pathways and, although aerobic respiration is preferred because of the highly favorable energetics of oxygen reduction, respiration can proceed in the absence of oxygen [1]. Fumarate represents one of the more common alternative terminal electron acceptors [2] and is reduced to succinate during anaerobic respiration by quinol-fumarate reductase (QFR), an integral membrane protein located in the bacterial periplasmic membrane. A pool of reduced quinones in the membrane serves as the electron source for fumarate reduction by QFR. The reduced quinones are ultimately generated through the action of an integral membrane protein donor, such as hydrogenase or a formate dehydrogenase.

For comparison, mitochondrial aerobic respiration [3] requires four integral membrane proteins: NADH-ubiquinone oxidoreductase (complex I); succinate-quinone

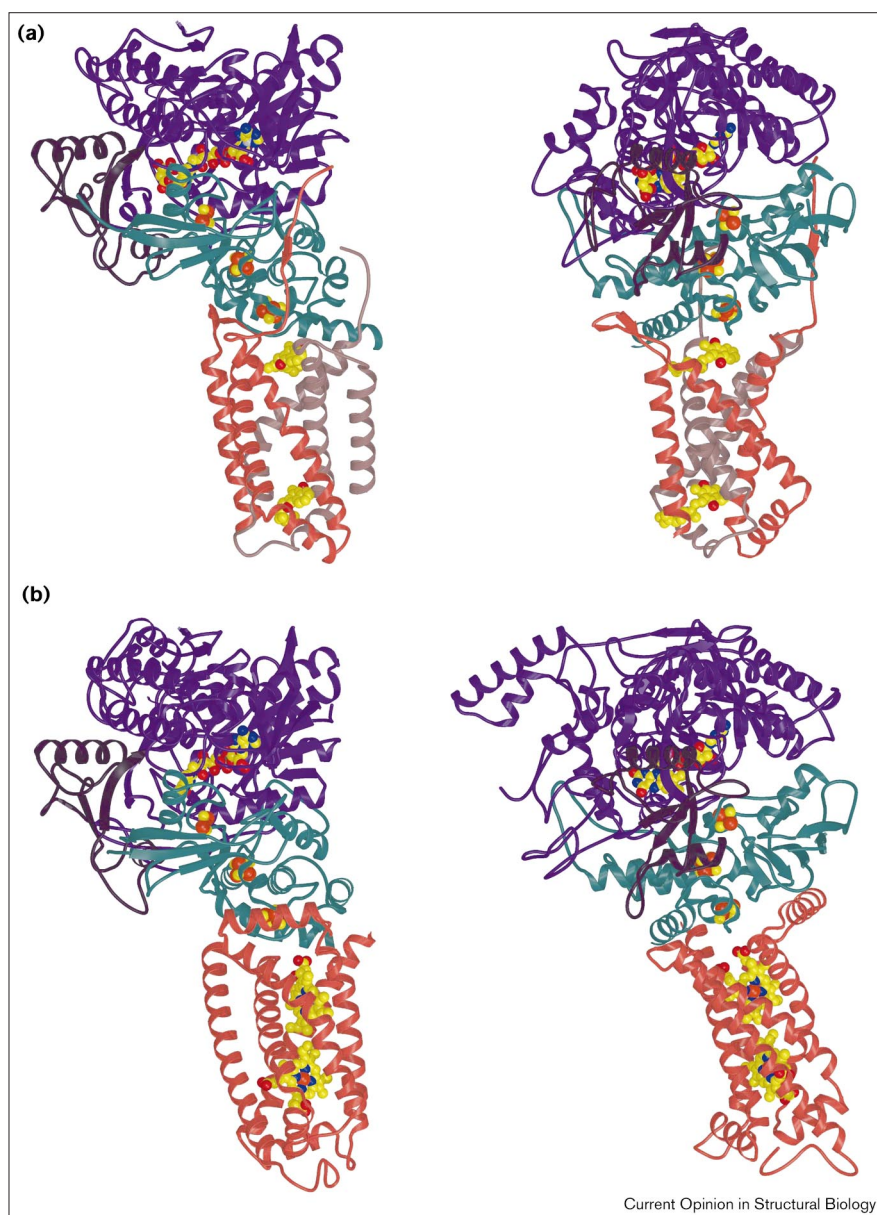
oxidoreductase (SQR; complex II); cytochrome *bc*<sub>1</sub> (complex III); and cytochrome *c* oxidase (complex IV); as well as the involvement of soluble cytochrome *c* and the ubiquinone pool to transport electrons between complexes. SQR and QFR represent a common element of both aerobic and anaerobic respiration, as they exhibit significant sequence similarity to one another. Both complexes can catalyze either the oxidation of succinate or the reduction of fumarate [4–6], although, physiologically, they function to catalyze this reaction in opposite directions [7–9]. In addition to its involvement in both aerobic and anaerobic respiration, complex II (SQR) also participates in the citric acid cycle, reflecting the central importance of this enzyme in basic metabolism [10].

QFR and SQR are composed of three or four subunits: the flavoprotein; the iron protein; and one or two transmembrane subunits, depending on the organism. The total molecular weight of a single complex is approximately 120 kDa. Both QFR and SQR can be separated into two components: a water-soluble domain and the membrane anchor subunit(s). The purified soluble domain consists of the flavoprotein subunit and the iron protein subunit, and retains catalytic activity for fumarate reduction when a suitable source of reducing equivalents is provided [11,12]. The subunits of the soluble domain exhibit strong sequence conservation throughout all species and contain a variety of redox cofactors. The flavoprotein contains FAD covalently linked to the Nε atom of a conserved histidine residue [13], whereas the iron protein contains three iron–sulfur clusters: a [2Fe–2S] cluster, a [3Fe–4S] cluster and a [4Fe–4S] cluster [7]. In contrast to the soluble subunits, the sequence and cofactor composition of the membrane anchor subunits vary among different organisms and even between QFR and SQR from the same organism. These membrane anchors have been assigned to four classes [14] that differ in the number of transmembrane subunits (one [designated subunit C] or two [designated subunits C and D]), the number of transmembrane helices (five or six) and the number of associated *b*-type heme moieties (zero, one or two).

The preceding year has witnessed an explosion in our structural understanding of complex II, with structures for the complete QFR complex from both *E. coli* [15••] and *Wolinella succinogenes* [16••] reported. Additionally, the structures of four soluble homologs of the flavoprotein subunit were described [17•–20•], which allows a detailed comparison of flavoprotein structure and increased insight into catalysis by complex II.

**Figure 1**

Ribbon diagrams of the (a) *E. coli* (PDB code 1FUM) and (b) *W. succinogenes* (PDB code 1QLA) QFR complexes. The flavoprotein is colored purple, with the capping domain highlighted in dark purple; the iron protein is colored teal; the C subunit membrane anchor is in peach; and the D subunit membrane anchor is in gray (*E. coli* enzyme only). Cofactors for both enzymes are shown as space-filling models, with carbon and sulfur in yellow, oxygen in red, nitrogen in blue and iron in orange. The left panel shows a view that is rotated 90° from the right panel. The *W. succinogenes* enzyme contains a C-terminal extension of the flavoprotein (b, right panel) that was not observed in the *E. coli* structure. Figures 1–3 and 5–7 were made using MOLSCRIPT [52], BOBSCRIPT [53], and RASTER3D [54].



Current Opinion in Structural Biology

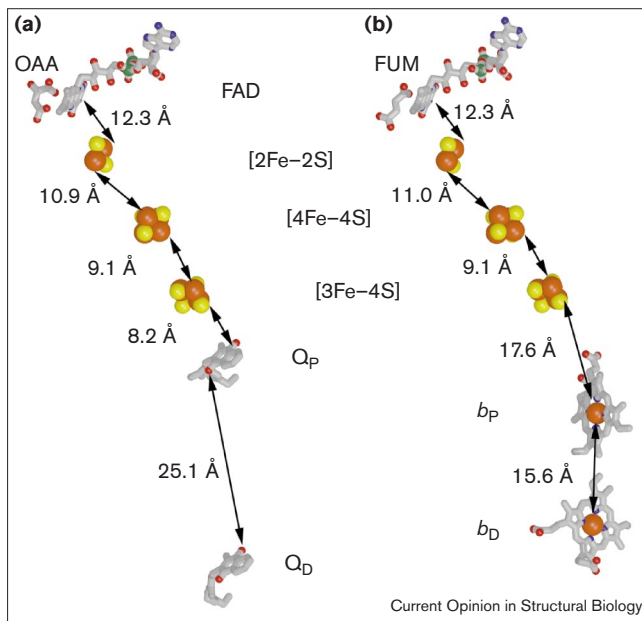
### Organization of the complex

As predicted from biochemical and sequence analyses, complex II exists as an essentially modular protein (Figure 1). Each subunit in the soluble domain exhibits homology to other known proteins, suggesting that the formation of this complex may have proceeded by the assembly of other proteins [21]. For example, soluble homologs of the flavoprotein have been seen in multiple pathways (NADH biosynthesis and fumarate reduction) and the iron protein exhibits sequence and structural similarity to both plant and bacterial ferredoxins. Furthermore, the iron protein exhibits weak sequence homology and similar cluster characteristics to iron protein subunits found in other terminal respiratory complexes, including the multisubunit membrane-bound dimethyl

sulfoxide reductase [22] and heterodisulfide reductase [23]. Thus, modular complex formation may represent an evolutionary mechanism for adjusting to the availability of dissimilar terminal electron acceptors.

In the transmembrane region, the membrane anchor subunits of the *E. coli* and *W. succinogenes* QFR complexes are organized around a central four-helix bundle, with two or one additional helices outside this central core, respectively. The *E. coli* and *W. succinogenes* QFRs (Figure 1) contain different cofactors associated with the membrane-spanning helices. In the *E. coli* QFR structure, two menaquinone molecules have been identified in the electron density, whereas the *W. succinogenes* enzyme contains two *b*-type hemes. As a result of the varied cofactor composition in the

Figure 2



Distances between cofactors in the (a) *E. coli* and (b) *W. succinogenes* QFR complexes. OAA and FUM are the inhibitor oxaloacetate and substrate fumarate, respectively, which are observed near the FAD in these structures. Carbon atoms are colored gray, oxygens are red, nitrogens are blue, sulfurs are yellow and irons are orange. Distances between redox centers are measured between the closest redox active atom of each cluster, rather than the center-to-center distance, as given in Iverson *et al.* [15\*\*]. The distances to hemes are measured to the edge of the porphyrin ring. The distances between cofactors in the soluble domains ([Fe-S] clusters and FAD) are conserved, whereas the distances between cofactors associated with the membrane anchors vary as a result of the differences in cofactor composition.

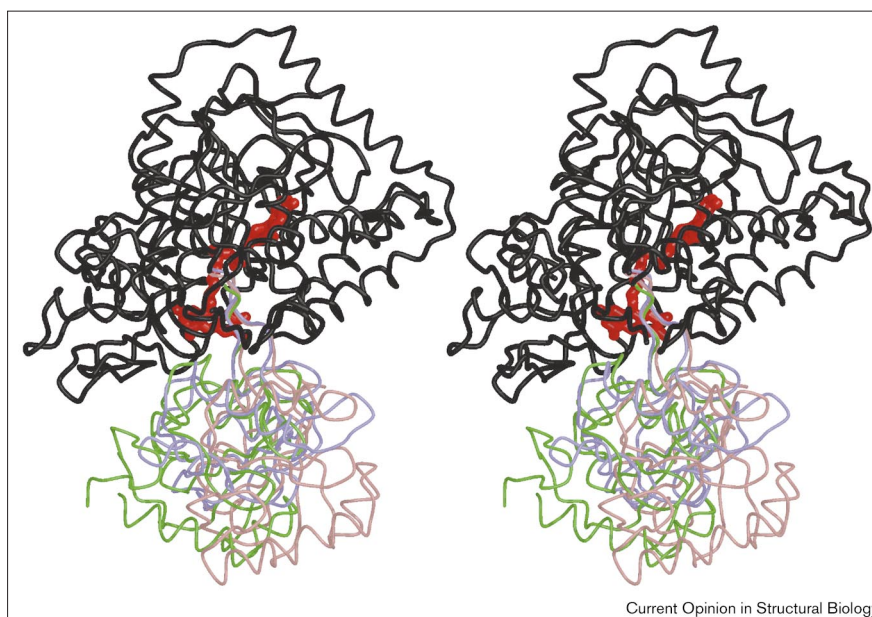
transmembrane region, the intercofactor distances (Figure 2) differ between the *E. coli* and *W. succinogenes* enzymes in the membrane-spanning region. This situation may be contrasted with the conserved distances between cofactors in the soluble domain.

In the crystal structures of both the *E. coli* and the *W. succinogenes* QFRs, two complexes are present in the asymmetric unit that associate through their transmembrane regions in a fashion suggestive of dimer formation. In the *E. coli* structure, this crystal contact buries 325 Å<sup>2</sup> of surface area and is mediated by two ordered detergent molecules (C<sub>12</sub>E<sub>9</sub>) [15\*\*]. In the *W. succinogenes* QFR structure, almost 3700 Å<sup>2</sup> of surface area is buried [16\*\*] in this interface, suggesting that this enzyme exists as a dimer. Although detergent molecules may have disassociated a physiological dimer in the *E. coli* enzyme, the C<sub>12</sub>E<sub>9</sub> detergent used in crystallization yields optimal enzyme activity when used in biochemical assays [24]. Additionally, it is possible that the crystals of the *W. succinogenes* enzyme contain a deceptively tight crystal contact and that the enzyme is indeed a monomer. On the basis of the intercofactor distances of the crystal packing interaction, if the *W. succinogenes* enzyme exists as a dimer, it probably acts as a structural, not a functional, dimer, unlike the situation in the cytochrome bc<sub>1</sub> complex [25–27].

### Fumarate reduction by the flavoprotein subunit and comparison of flavoprotein conformations

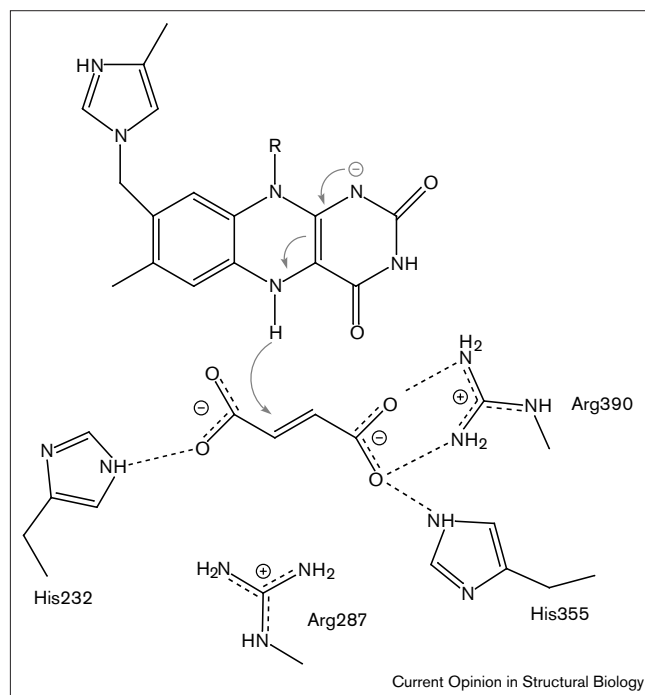
The flavoprotein subunit contains two major domains: a flavin-binding domain based on a Rossmann-type fold and a capping domain (Figure 1). The flavin-binding domain exhibits sequence and structural conservation among the two full-length QFR structures (*E. coli* and *W. succinogenes*),

Figure 3



Stereo view illustrating the movement of the capping domain with respect to the flavin-binding domain in the flavoprotein subunit of recently solved structures of fumarate reductase flavoproteins. The capping domains from the *S. putrefaciens* (green; PDB code 1D4D; [19\*]), *S. frigidimarina* (pink; PDB code 1QO8; [18\*]) and *W. succinogenes* (lilac; PDB code 1QLA; [16\*\*]) flavoenzymes are shown relative to a least squares superposition of their flavin-binding domains (black), with the position of the FAD indicated (red). The maximal displacement of the capping domain suggests that the hinge connecting the two domains can bend by more than 30°. Other flavoproteins with intermediate hinge angles have been omitted for clarity.

Figure 4



Schematic diagram of active site interactions with the proposed reaction mechanism of fumarate reductase. Hydrogen bond interactions between the protein and bound ligand are indicated (dashed lines), with the exception of Arg287, which exhibits significant conformational variability in the different structure determinations. Hydride transfer from N5 of FAD (gray arrows) represents the initial step of fumarate reduction, followed by proton transfer to the substrate. The sidechains of His232, Arg287, His355 and Arg390 are possible candidates for the immediate proton donor. Arg287 and Arg390 have also been shown to be necessary for covalent attachment of the FAD to His44 (E Maklashina, I Schröder, G Cecchini, unpublished data).

the soluble fumarate reductases [18<sup>•</sup>–20<sup>•</sup>] and L-aspartate oxidase (LASPO) [17<sup>•</sup>]. The pairwise deviations among C $\alpha$  atoms in these proteins never exceed 1.7 Å, consistent with a sequence identity that is never less than 30%.

The flavin-binding domain and capping domain of the flavoprotein are connected by a small hinge region consisting of two  $\beta$  strands, with the active site located at the interface between these two domains. An overlay of recently solved structures containing the flavoprotein fold [17<sup>•</sup>–20<sup>•</sup>,28] shows that the relative angle between the flavin-binding and capping domains can vary (Figure 3).

It is proposed that, during catalysis, fumarate enters the active site, with concomitant closure of the capping domain, sterically causing a rotation of the substrate carboxylate around the double bond (Figure 4). Bound substrate has been shown to be distorted in complexes with the *W. succinogenes* enzyme [16<sup>••</sup>] and the soluble *Shewanella* enzyme [19<sup>•</sup>]. Fumarate reduction then proceeds by hydride transfer from the N5 of the flavin, followed by proton transfer from a nearby sidechain. Four

active site residues (His232, Arg287, His355 and Arg390 in the *E. coli* sequence) that directly contact the substrate or inhibitor are absolutely conserved in all available sequences. Three of these residues, His232, Arg287 and Arg390, have been substituted by site-directed mutagenesis and are known to be critical for enzyme activity ([29]; E Maklashina, I Schröder, G Cecchini, unpublished data). Both His355 and Arg390 have been suggested as proton donors for this reaction [16<sup>••</sup>,19<sup>•</sup>]; however, the role each sidechain plays in the reaction mechanism remains to be conclusively established.

In an overlay of the ensemble of available structures (Figure 5), the sidechains of His232, His355 and Arg390 appear to be structurally conserved in terms of both location and conformation. In contrast, Arg287, which is located in the capping domain, exhibits different conformations, depending on both the orientation of the capping domain and the nature of the species bound at the active site. This suggests that Arg287 may be involved in recruiting the substrate into or moving the product out of the active site.

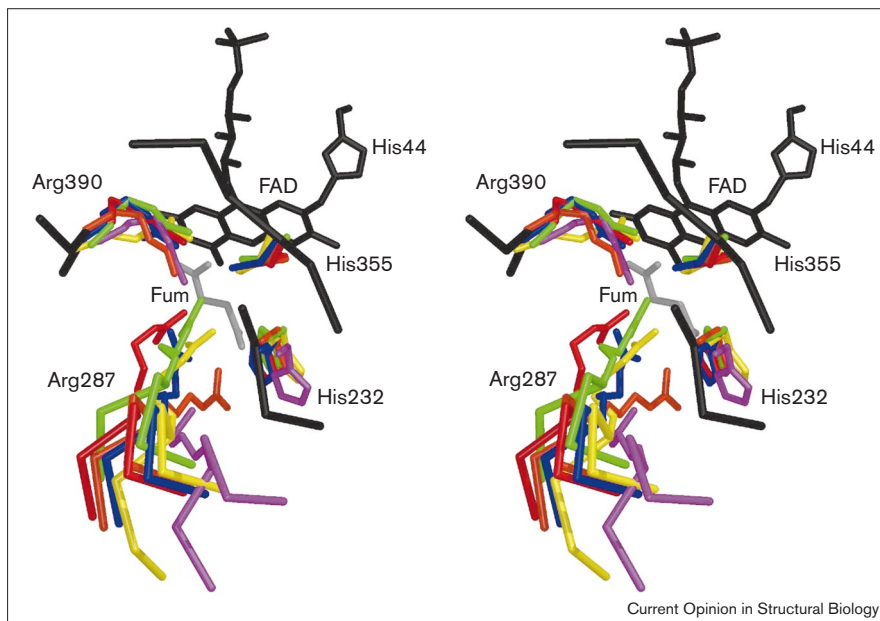
### The iron protein

As predicted by sequence similarity to plant and bacterial ferredoxins, the iron protein contains two domains. The N terminus has a fold similar to plant-type ferredoxins surrounding the [2Fe–2S] cluster, whereas the C-terminal domain exhibits a core similar to that of bacterial ferredoxins and contains the cysteine ligands to the [4Fe–4S] and [3Fe–4S] clusters. The C-terminal domain additionally contains several other helices that associate with the membrane anchor subunits. In agreement with electron paramagnetic resonance (EPR) spectroscopy [30–33], the three clusters are arranged in a nearly linear fashion, leading from the membrane anchor to the active site flavin (Figure 2). This structural organization indicates that, despite the low reduction potential of the [4Fe–4S] cluster [7,8], it is probable that all the [Fe–S] clusters participate in electron transfer between the quinone pool and fumarate [34<sup>••</sup>,35<sup>••</sup>].

### Organization of cofactors in the membrane: a possible role in energy transduction

Two sets of transmembrane-associated cofactors are present in the two available QFR structures: two menaquinone molecules (Q<sub>P</sub> and Q<sub>D</sub>, where Q<sub>P</sub> is the menaquinone proximal to the QFR soluble domain and Q<sub>D</sub> is the menaquinone distal to the QFR soluble domain) are observed in the *E. coli* enzyme, whereas two *b*-type hemes (*b*<sub>P</sub> and *b*<sub>D</sub>) bind to the *W. succinogenes* enzyme (Figure 1). Despite the differences in subunit composition, sequences and cofactor components, the transmembrane anchors of the *E. coli* and *W. succinogenes* QFRs are both organized around an antiparallel four-helix bundle in the membrane, with two or one additional peripheral transmembrane helices, respectively. In each structure, one of the helices of the four-helix bundle contains a distinctive bend in the transmembrane section. As an ideal four-helix bundle is twofold symmetric, the transmembrane helices

Figure 5

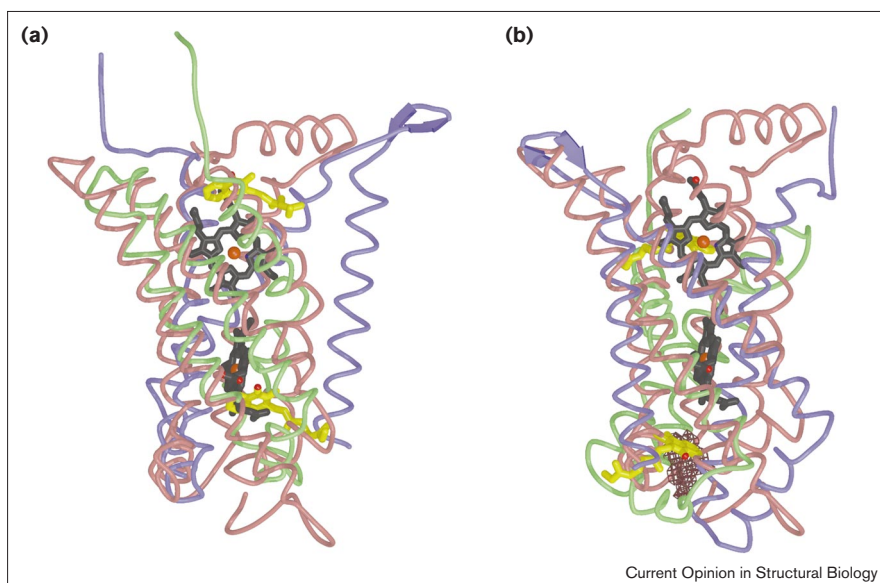


Stereo view illustrating the superposition of active site residues from different fumarate reductase structures. The positions of residues from the *E. coli* (PDB code 1FUM) enzyme are in red, those from the *W. succinogenes* (PDB code 1QLB) enzyme are in orange, those from *L*-aspartate oxidase (PDB code 1CHU) are in yellow, those from the *S. frigidimarina* soluble fumarate reductase are in green and blue (PDB codes 1QO8 and 1QJD, respectively) and those from the *S. putrefaciens* fumarate reductase (PDB code 1D4D) are in magenta. The cofactor FAD and substrate fumarate (Fum) are black and gray, respectively. Although the positions of His232, His355 and Arg390 are structurally conserved, the positions of the Arg287 sidechain and the surrounding mainchain are more variable.

of the QFR structures can be aligned in two distinct ways. In one alignment, the C subunit of the *E. coli* enzyme is superimposed with the N terminus of the C subunit of the *W. succinogenes* enzyme, yielding an rmsd of 2.4 Å for 113 C $\alpha$  atoms between corresponding residues in the five transmembrane helices of the *Wolinella* and *E. coli* enzymes. In this alignment, the connections between the transmembrane helices are similar and the bent helices superimpose (Figure 6a). If the menaquinone molecules from the *E. coli* QFR were transferred into the *W. succinogenes* enzyme, however, they would sterically clash with the

distal heme of the latter enzyme. In the second alignment, which is rotated approximately 180° from the first alignment, the N terminus of the D subunit of the *E. coli* enzyme becomes superimposed with the N terminus of the C subunit of the *W. succinogenes* enzyme (Figure 6b). Although this alignment appears to be quantitatively inferior (rmsd 2.2 Å for only 62 C $\alpha$  atoms), it preserves the relative orientation between the transmembrane helices and the soluble domains in the two QFR structures. Furthermore, the Q<sub>D</sub> menaquinone from the *E. coli* enzyme no longer sterically clashes with the distal heme,

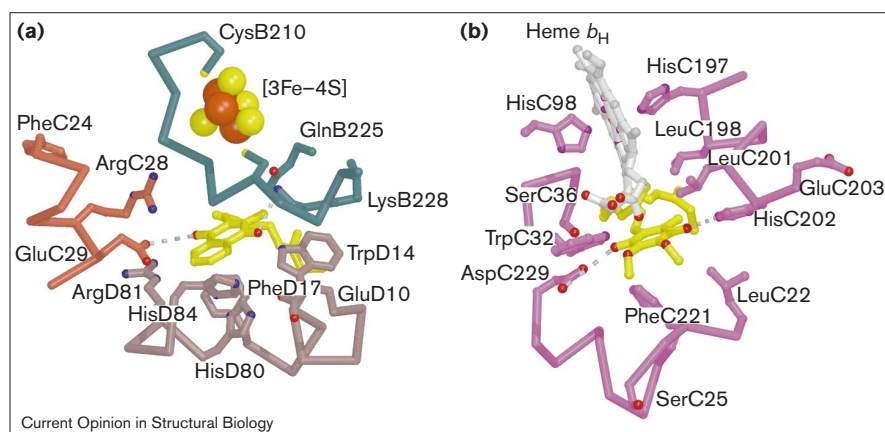
Figure 6



Alignment of transmembrane helices from the *E. coli* (PDB code 1FUM) and *W. succinogenes* (PDB code 1QLB) QFR complexes. (a) Superposition of the transmembrane helices of the N terminus of the C subunit from the *E. coli* enzyme (C subunit in lilac and D subunit in green) with the N terminus of the C subunit from the *W. succinogenes* enzyme (pink). Quinones from the *E. coli* enzyme are shown in yellow, whereas the hemes from the *Wolinella* enzyme are in black. The heme iron and quinone oxygens are represented by red spheres. (b) Alternate alignment superimposing the N terminus of the *E. coli* enzyme D subunit with the N terminus of the *W. succinogenes* C subunit. A cavity located using the program VOIDOO [55] in the *W. succinogenes* enzyme is shown in brown mesh. If this cavity represents a quinone-binding site for the *Wolinella* enzyme, the location of the Q<sub>D</sub> site would be structurally preserved in both enzymes.

**Figure 7**

Quinone-binding environments in respiratory complexes. **(a)** Binding pocket for  $Q_p$  in the *E. coli* QFR reductase complex. The quinone-binding environment includes hydrogen bonds to the sidechains of GluC29 and LysB228. The color scheme is the same as in Figure 1, with hydrogen bonds indicated by dashed lines. **(b)** Binding pocket for  $Q_i$  in the chicken cytochrome  $bc_1$  complex [26; PDB code 1BCC). The structural arrangement of the hydrogen bonds relative to the quinone shows similarities to that seen in *E. coli* QFR. Additionally, several other residue pairs (PheD17 [QFR] and PheC221 [ $bc_1$ ]; TrpD14 [QFR] and LeuC22 [ $bc_1$ ]; [3Fe-4S] [QFR] and heme  $b_H$  [ $bc_1$ ]) occupy similar positions relative to the quinones in these two structures.



suggesting that this position might correspond to where  $Q_D$  could bind in the *W. succinogenes* enzyme. Indeed, a cavity is present in *Wolinella* QFR near this position that might represent the cofactor-binding site for this complex.

The separation distance between the two menaquinone molecules in the *E. coli* enzyme is approximately 25 Å (Figure 2). While electron transfer has been observed between centers separated by approximately 25 Å in proteins [36••], redox cofactors are typically spaced by no more than half this distance [34••]. Although this could indicate that the  $Q_D$  site is not catalytically relevant, an alternative explanation is that a third cofactor-binding site is positioned between the  $Q_p$  and  $Q_D$  sites and would be approximately 13 Å from each of the established quinone-binding sites [35••]. Although the involvement of an additional cofactor cannot be conclusively proven, several factors point to its possible existence. Biochemical evidence [37–39] suggests that  $Q_D$  is necessary for physiological catalysis and site-directed mutagenesis has implicated a cluster of residues between the two known quinone-binding sites as necessary for enzyme function [37]. This cluster of residues lies near a cavity between the transmembrane helices in the *E. coli* enzyme and is associated with density from the structure determination that could not be assigned. Spectroscopic evidence suggests that a stabilized semiquinone pair separated by approximately 8 Å is localized near the [3Fe-4S] cluster [33,40–43], which could be a result of  $Q_p$  interacting with a quinone in a central binding site that could not be identified in the density. Indeed, several residues (TrpC86, ArgD51) lining the pocket of the potential quinone-binding site also line the  $Q_p$ -binding site. Although a menaquinone molecule could not be docked into the density observed in the *E. coli* structure determination, it is possible that this site is only partially occupied in the crystal structure.

One intriguing observation concerning the quinone locations in *E. coli* QFR is that they are positioned on opposite sides of the membrane, as observed for the two quinone-binding sites in the cytochrome  $bc_1$  complex [25–27]. In

cytochrome  $bc_1$ , this transmembrane arrangement is essential for proton pumping across the mitochondrial membrane via a  $Q$ -cycling mechanism [44]. In addition to the similar locations of the quinone-binding sites, the environment of the  $Q_p$  site (Figure 7a) has certain features in common with the  $Q_o$  (quinol-oxidizing) and  $Q_i$  (quinone-reducing) (Figure 7b) sites of cytochrome  $bc_1$ . Proton translocation at the  $Q_o$  site in cytochrome  $bc_1$  is thought to occur through the Rieske center ligand His161 and GluC271 (bovine numbering). These two residues only form hydrogen bonds to inhibitors when the Rieske iron-sulfur center is positioned near the  $Q_o$  site ([45; S Iwata, personal communication), thereby mechanically coupling proton translocation to electron transfer to the Rieske center. Analysis of the  $Q_i$  site suggests that the conserved AspC229 and HisC202 residues (chicken numbering), both of which form hydrogen bonds to the quinone (Figure 7b), participate in the proton translocation mechanism. In the *E. coli* QFR structure, GluC29 and LysB228 are each within hydrogen bonding distance of the quinone (Figure 7a). GluC29 has been shown by site-directed mutagenesis [37] to be critical to enzyme function. The thermodynamic basis for energy coupling through QFR has been detailed in [35••]. If other modular terminal respiratory acceptors, such as dimethyl sulfoxide reductase or heterodisulfide reductase, have evolved with a similar transmembrane arrangement of quinone-binding sites, it is possible that these proteins may employ a  $Q$ -cycling mechanism to pump protons.

## Conclusions

Structural information is now available for most members of the aerobic respiratory chain, including atomic-level resolution crystal structures of respiratory complexes II–IV [25–27,46,47] and much of the ATP synthase [48,49••], and electron microscopic reconstruction of complex I [50,51] at approximately 30 Å resolution. In the past year, structures have been reported for two full-length QFRs, one from *E. coli* [15••] and one from *W. succinogenes* [16••], as well as for several soluble homologs [17•–20•]. This ensemble of

fumarate reductase structures allows a better understanding of the reaction mechanism catalyzed by the flavoprotein, as well as an understanding of how electrons are passed from the membrane soluble quinones into the active site of the enzyme. Additionally, these structures open the question of whether QFR can potentially couple electron transfer to proton translocation, thereby representing an additional mechanism for energy conservation in respiratory chains.

## Acknowledgements

This work has been supported by the Department of Veterans Affairs (GC) and funding from the Howard Hughes Medical Institute (DCR), National Institutes of Health grants GM45162 (DCR) and HL-16251 (GC), and National Science Foundation grant MCB-9729778 (GC). We would like to acknowledge stimulating discussions with T Ohnishi, PL Dutton, HB Gray and S Iwata.

## References and recommended reading

Papers of particular interest, published within the annual period of review, have been highlighted as:

- of special interest
- of outstanding interest

1. Hederstedt L: **Respiration without O<sub>2</sub>**. *Science* 1999, **284**:1941-1942.
  2. Kröger A, Geisler V, Lemma E, Theis F, Lenger R: **Bacterial fumarate respiration**. *Arch Microbiol* 1992, **158**:311-314.
  3. Saraste M: **Oxidative phosphorylation at the fin de siècle**. *Science* 1999, **283**:1488-1493.
  4. Guest JR: **Partial replacement of succinate dehydrogenase function in phage and plasmid-specified fumarate reductase in *Escherichia coli***. *J Gen Microbiol* 1981, **122**:171-179.
  5. Maklashina E, Berthold DK, Cecchini G: **Anaerobic expression of *Escherichia coli* succinate dehydrogenase: functional replacement of fumarate reductase in the respiratory chain during anaerobic growth**. *J Bacteriol* 1998, **180**:5989-5996.
  6. Pershad HR, Hirst J, Cochran B, Ackrell BAC, Armstrong FA: **Voltammetric studies of bidirectional catalytic electron transport in *Escherichia coli* succinate dehydrogenase: comparison with the enzyme from beef heart mitochondria**. *Biochim Biophys Acta* 1999, **1412**:262-272.
  7. Ackrell BAC, Johnson MK, Gunsalus RP, Cecchini G: *Chemistry and Biochemistry of Flavoenzymes*, vol III. Edited by Müller F. Boca Raton: CRC Press; 1992:229-297.
  8. Hägerhäll C: **Succinate:quinone oxidoreductases. Variations on a conserved theme**. *Biochim Biophys Acta* 1997, **1320**:107-141.
  9. Hellemond JJV, Tielens AGM: **Expression and functional properties of fumarate reductase**. *Biochem J* 1994, **304**:321-331.
  10. Guest JR, Russell GC: **Complexes and complexities of the citric acid cycle in *Escherichia coli***. *Curr Top Cell Regul* 1992, **33**:231-247.
  11. Singer TP, Kearney EB, Kenney WC: **Succinate dehydrogenase**. *Adv Enzymol* 1973, **37**:189-272.
  12. Ackrell BAC, Kearney EB, Singer TP: **Mammalian succinate dehydrogenase**. *Methods Enzymol* 1978, **53**:466-483.
  13. Walker WH, Singer TP: **Identification of the covalently-bound flavin of succinate dehydrogenase as 8 $\alpha$ -(histidyl) flavin adenine dinucleotide**. *J Biol Chem* 1970, **245**:4224-4225.
  14. Hägerhäll C, Hederstedt L: **A general structural model for the membrane-domain of succinate:quinone oxidoreductases**. *FEBS Lett* 1996, **389**:25-31.
  15. Iverson TM, Luna-Chavez C, Cecchini G, Rees DC: **Structure of the *Escherichia coli* fumarate reductase respiratory complex**. *Science* 1999, **284**:1961-1966.
- This first structural analysis of quinol-fumarate reductase details the organization of the complex and reveals bound quinones in the membrane-spanning regions. The locations of these quinones are reminiscent of quinones involved in energy transduction.
16. Lancaster CRD, Kröger A, Auer M, Michel H: **Structure of fumarate reductase from *Wolinella succinogenes* at 2.2 Å resolution**. *Nature* 1999, **402**:377-385.
- The structure determination of intact quinol-fumarate reductase (QFR) from *W. succinogenes* allows the analysis of *b*-type hemes bound to the membrane anchor subunit and reveals common elements of QFR structure through comparisons with the *E. coli* enzyme.
17. Mattevi A, Tedeschi G, Bacchella L, Coda A, Negri A, Ronchi S:
    - **Structure of L-aspartate oxidase: implication for the succinate dehydrogenase/fumarate reductase oxidoreductase family**. *Structure* 1999, **7**:745-756.
- The first structure determination of a soluble homolog of the fumarate reductase flavoprotein suggests that flexibility exists between the flavin-binding domain and the capping domain.
18. Bamford V, Dobbin PS, Richardson DJ, Hemmings AM: **Open conformation of a flavocytochrome c<sub>3</sub> fumarate reductase**. *Nat Struct Biol* 1999, **6**:1104-1109.
- See annotations to [19\*,20\*].
19. Leys D, Tsapin AS, Nealsen KH, Meyer TE, Cusanovich MA, VanBeeumen JJ: **Structure and mechanism of the flavocytochrome c fumarate reductase of *Shewanella putrefaciens* MR-1**. *Nat Struct Biol* 1999, **6**:1113-1117.
- See annotations to [18\*,20\*].
20. Taylor P, Pealing SL, Reid GA, Chapman SK, Walkinshaw MD:
    - **Structural and mechanistic mapping of a unique fumarate reductase**. *Nat Struct Biol* 1999, **6**:1108-1112.
- This paper, together with [18\*,19\*], reports the structure determination of soluble fumarate reductases. Published simultaneously, these papers provide further support for the occurrence of domain movement in the flavoprotein.
21. Gest H: **The evolution of biological energy-transducing systems**. *FEMS Lett* 1980, **7**:73-77.
  22. Bilous PT, Cole ST, Andersib WF, Weiner JH: **Nucleotide sequence of the *dmsABC* operon encoding the anaerobic dimethylsulphoxide reductase of *Escherichia coli***. *Mol Microbiol* 1988, **2**:785-795.
  23. Künkel A, Vaupel M, Heim S, Thauer RK, Hedderich R: **Heterodisulfide reductase from methanol-grown cells of *Methanosarcina barkeri* is not a flavoenzyme**. *Eur J Biochem* 1997, **244**:226-234.
  24. Luna-Chavez C, Iverson TM, Rees DC, Cecchini G: **Overexpression, purification, and crystallization of the membrane-bound fumarate reductase from *Escherichia coli***. *Protein Expr Purif* 2000, **19**:186-196.
  25. Xia D, Yu C, Kim H, Xia J, Kachurin AM, Zhang L, Yu L, Deisenhofer J: **Crystal structure of the cytochrome bc<sub>1</sub> complex from bovine heart mitochondria**. *Science* 1997, **277**:60-66.
  26. Zhang Z, Huang L, Schulmeister VM, Chi YI, Kim KK, Hung LW, Crofts AR, Berry EA, Kim S-H: **Electron transfer by domain movement in cytochrome bc<sub>1</sub>**. *Nature* 1998, **392**:677-684.
  27. Iwata S, Lee JW, Okada K, Lee JK, Iwata M, Rasmussen B, Link TA, Ramaswamy S, Jap BK: **Complete structure of the 11-subunit bovine mitochondrial bc<sub>1</sub> complex**. *Science* 1998, **281**:64-71.
  28. Ackrell BAC: **Progress in understanding structure-function relationships in respiratory chain complex II**. *FEBS Lett* 2000, **466**:1-5.
  29. Schröder I, Gunsalus R, Ackrell BAC, Cochran B, Cecchini G: **Identification of active site residues of *Escherichia coli* fumarate reductase by site directed mutagenesis**. *J Biol Chem* 1991, **266**:13572-13579.
  30. Morningstar JE, Johnson MK, Cecchini G, Ackrell BAC, Kearney EB: **The high-potential iron-sulfur center in *Escherichia coli* fumarate reductase is a 3-iron cluster**. *J Biol Chem* 1985, **260**:3631-3638.
  31. Cammack R, Patil DS, Weiner JH: **Evidence that center-2 in *Escherichia coli* fumarate reductase is a [4Fe-4S] cluster**. *Biochim Biophys Acta* 1986, **870**:545-551.
  32. Kowal AT, Werth MT, Manodori A, Cecchini G, Schröder I, Gunsalus RP, Johnson MK: **Effect of cysteine to serine mutation on the properties of the [4Fe-4S] center in *Escherichia coli* fumarate reductase**. *Biochemistry* 1995, **34**:12284-12293.
  33. Waldeck AR, Stowell MHB, Lee HK, Hung SC, Matsson M, Hederstedt L, Ackrell BAC, Chan SI: **Electron paramagnetic resonance studies of succinate:ubiquinone oxidoreductase from *Paracoccus denitrificans***. *J Biol Chem* 1997, **272**:19373-19382.

34. Page CC, Moser CC, Chen X, Dutton PL: **Natural engineering principles of electron tunneling in biological molecules.** *Nature* 1999, **402**:47-52.  
This thorough compilation of electron transfer proteins discusses the mechanism of endergonic tunneling, as well as explaining the biological tendency for redox cofactors to be positioned at distances approximately 13 Å apart in proteins.
35. Ohnishi T, Moser CC, Page CC, Dutton PL, Yano T: **Simple redox-linked proton-transfer design: new insights from structures of quinol-fumarate reductase.** *Structure* 2000, **8**:R23-R32.  
This insightful mini-review focuses on the bioenergetics of quinol-fumarate reductase and succinate-quinone oxidoreductase.
36. Winkler JR, DiBilio A, Farrow NA, Richards JH, Gray HB: **Tunneling in biological molecules.** *Pure Appl Chem* 1999, **71**:1753-1764.  
A comparison of electron tunneling rates in Ru-modified heme and copper-containing proteins reveals that the structure of the intervening polypeptide ( $\alpha$  helix or  $\beta$  strand) between the donor and acceptor affects the rate of electron transfer.
37. Westenberg DJ, Gunsalus RP, Ackrell BAC, Sices H, Cecchini G: **Escherichia coli fumarate reductase FrdC and FrdD mutants. Identification of amino acid residues involved in catalytic activity with quinones.** *J Biol Chem* 1993, **268**:815-822.
38. Lee GY, He DY, Yu L, Yu CA: **Identification of the ubiquinone-binding domain in QPs1 of succinate-ubiquinone reductase.** *J Biol Chem* 1995, **270**:6193-6198.
39. Shenoy SK, Yu L, Yu CA: **The smallest membrane anchoring subunit (QPs3) of bovine heart mitochondrial succinate-ubiquinone reductase. Cloning, sequencing, topology, and Q-binding domain.** *J Biol Chem* 1997, **272**:17867-17872.
40. Salerno JC, Harmon HJ, Blum H, Leigh JS, Ohnishi T: **A transmembrane quinone pair in the succinate dehydrogenase cytochrome b region.** *FEBS Lett* 1977, **82**:179-182.
41. Rich PR, Moore AL, Ingledew WJ, Bonner WDJ: **EPR studies of higher plant mitochondria. I Ubisemiquinone and its relation to alternative respiratory oxidations.** *Biochim Biophys Acta* 1977, **504**:345-363.
42. Rich PR, Bonner WDJ: **An EPR analysis of cyanide-resistant mitochondria isolated from the mutant poky strain of Neurospora crassa.** *Biochim Biophys Acta* 1978, **504**:345-363.
43. Salerno JC, Ohnishi T: **Studies on the stabilized ubisemiquinone species in the succinate-cytochrome c reductase segment of the intact mitochondrial membrane system.** *Biochem J* 1980, **192**:769-781.
44. Mitchell P: **Coupling of phosphorylation to electron and hydrogen transfer by a chemi-osmotic type of mechanism.** *Nature* 1961, **191**:144-148.
45. Crofts AR, Barquera B, Gennis RB, Kuras R, Guergova-Kuras M, Berry EA: **Mechanism of ubiquinol oxidation by the bc<sub>1</sub> complex: different domains of the quinol binding pocket and their role in the mechanism and binding of inhibitors.** *Biochemistry* 1999, **38**:15807-15826.
46. Iwata S, Ostermeier C, Ludwig B, Michel H: **Structure at 2.8-Ångstrom resolution of cytochrome c oxidase from Paracoccus denitrificans.** *Nature* 1995, **376**:660-669.
47. Tsukihara T, Aoyama H, Tomizaki T, Yamaguchi H, Sinsawattho K, Nakashima R, Yaono R, Yoshikawa S: **The whole structure of the 13-subunit oxidized cytochrome c oxidase at 2.8 Ångstrom.** *Science* 1996, **272**:1136-1144.
48. Abrahams JP, Leslie AGW, Lutter R, Walker JE: **Structure at 2.8-Ångstrom resolution of F1ATPase from bovine heart-mitochondria.** *Nature* 1994, **370**:621-628.
49. Stock D, Leslie AGW, Walker JE: **Molecular architecture of the rotary motor in ATP synthase.** *Science* 1999, **286**:1700-1705.  
The determination of the structure of the ATP synthase, including the c subunits for the integral membrane F<sub>0</sub> component, shows a homodecameric arrangement of the c subunits associated with the trimeric water-soluble F<sub>1</sub> component, suggesting that a nonintegral number of protons are pumped for each ATP synthesized.
50. Guénebaud V, Vincentelli R, Mills D, Weiss H, Leonard KR: **Three dimensional structure of NADH-dehydrogenase from Neurospora crassa by electron microscopy and conical tilt reconstruction.** *J Mol Biol* 1997, **265**:409-418.
51. Grigorieff N: **Three-dimensional structure of bovine NADH:ubiquinone oxidoreductase (complex I) at 22 Å in ice.** *J Mol Biol* 1998, **277**:1033-1046.
52. Kraulis PJ: **MOLSCRIPT – a program to produce both detailed and schematic plots of protein structures.** *J Appl Crystallogr* 1991, **24**:946-950.
53. Esnouf R: **BOBSCRIPT – an extensively modified version of molscript that includes greatly enhanced coloring capabilities.** *J Mol Graph* 1997, **15**:133-138.
54. Merritt EA, Murphy MEP: **Raster3D Version 2.0 – a program for photorealistic molecular graphics.** *Acta Crystallogr* 1994, **D50**:869-873.
55. Kleywegt GJ, Jones TA: **Detection, delineation, measurement and display of cavities in macromolecular structures.** *Acta Crystallogr* 1994, **D50**:175-185.